FINITE ELEMENT ANALYSIS OF SRCMU MASONRY WALLS WITH NSM REINFORCEMENT IN OUT-OF-PLANE FLEXURE

Sparling, Adrien[1]; Palermo, Dan[2] and Hashemian, Fariborz[3]

ABSTRACT

In recent decades the use of conventional masonry in the area of light industrial warehouse construction has been replaced by other materials. This is attributed, in part, to the high cost of stiffening elements (i.e. columns or pilasters) required for the construction of freestanding masonry walls. The innovative Surface-Reinforced Concrete Masonry Unit (SRCMU) system, incorporating near-surface mounted (NSM) reinforcement, has demonstrated the potential to address current challenges in conventional masonry construction by enabling the construction of lighter and stiffer walls without requiring stiffening elements. SRCMUs are hollow concrete blocks that contain vertical groves on their exterior faces, allowing reinforcing bars to be placed near the extreme tension fibre of walls subjected to out-of-plane loads. To this end, a series of four masonry walls were recently constructed for testing under conditions of third-point flexural loading. The walls were constructed from 200 mm (nominal) hollow concrete masonry units, and have a width of 1.2 m and height of 3.2 m. Each wall contains the same gross vertical reinforcement ratio of 0.26%. The objective of the testing program is to isolate and determine the effect of grouting as well as that of reinforcing bar placement on out-of-plane flexural behaviour. Finite element analyses of NSM reinforced SRCMU walls are presented herein to illustrate the anticipated benefits of this system over conventional reinforced masonry.

KEYWORDS: *finite element analysis, flexural testing, light industrial warehouse, NSM reinforcement, SRCMU*

INTRODUCTION

Conventional reinforced masonry construction makes use of cementitious grout in order to bond reinforcing bars into the hollow cores of standard concrete masonry unit (CMU) assemblies. Given that hollow CMUs are approximately 50% void, the grouting process effectively doubles

[1]PhD Student, Civil Engineering, York University, 4700 Keele St., Toronto, ON, Canada, adriensp@yorku.ca
[2]Associate Professor, Civil Engineering, York University, 4700 Keele St., Toronto, ON, Canada, dan.palermo@lassonde.yorku.ca
[3]Adjunct Professor, Civil Engineering, York University, 4700 Keele St., Toronto, ON, Canada, fariborz.khaleghihashemian@pc.gc.ca

the weight of masonry assemblies when compared to the hollow assembly. Additionally, this method of reinforcing walls usually places reinforcing bars at or near the wall's out-of-plane neutral axis. This practice severely limits the cracked out-of-plane stiffness of a wall, and limits a designer's ability to control horizontal cracking.

In an attempt to maximize the effectiveness of vertical reinforcing bars, Abboud et al. [1] tested a staggered placement of reinforcing bars. Other researchers have studied the application of near-surface mounted (NSM) reinforcing materials to improve the strength of existing masonry structures, though most of these focus on improving the earthquake-resilience of unreinforced masonry structures [2].

Vertical grooves on the exterior surfaces of Surface-Reinforced Concrete Masonry Units (SRCMU) allow for the construction of masonry assemblies erected in running bond to have continuous vertical grooves along their entire height. These grooves are convenient for the placement of NSM reinforcing bars. By using this technique, tensile reinforcing materials can be located near the extreme tension fibre while the hollow cores of masonry assemblies remain hollow. Anticipated benefits of this construction technique over conventionally-reinforced masonry assemblies suggested by Sparling et al. [4] and Sparling [5] include the following: increased out-of-plane flexural stiffness, reduced assembled weight, and reduced construction time. The increased out-of-plane flexural stiffness, which may mitigate P-Δ effects and allow for the construction of taller slender reinforced masonry walls is currently investigated.

PROPOSED TESTING

The proposed testing includes four walls to be loaded out-of-plane to determine their flexural characteristics. These walls will be tested in third-point loading with no imposed axial load. Although this loading setup does not accurately reflect conditions in actual structures, it allows zones of maximum moment and maximum shear to be scrutinized separately. It also allows for the observation of the effects of varying moment and shear.

Materials

The CMUs for this series of tests were manufactured using commercial materials and manufacturing methods. Control walls were constructed from conventional 15MPa, 200mm (nominal values) stretcher units. SRCMUs were produced by modifying a typical mould used for conventional units. The cross section of conventional CMUs is shown alongside that of the SRCMU in Figure 1.
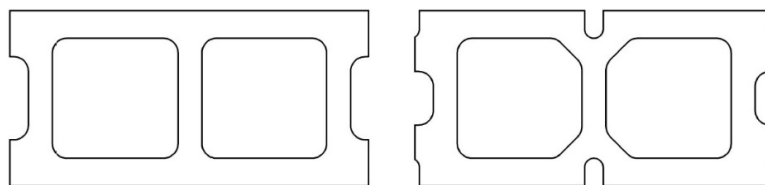

Figure 1: Typical Cross-Section of a Convention CMU (left) and a SRCMU (right)

Mortar for the construction of the walls was mixed from commercially available Type S premixed bagged mortar mix. Both 10M and 20M steel reinforcing bars were of 400 grade. Grout was prepared following CSA A179 with cement: fine aggregate: coarse aggregate proportions of 1:2.5:1.5 by volume. For the walls with NSM reinforcement, reinforcing bars were bonded to the masonry using a low-sag dowelling epoxy. All masonry walls and test prisms were constructed by a certified Red Seal journeyman mason.

Test Specimens

The cross section of the walls were selected in order to compare the effect of different reinforcing bar locations within the wall cross section, as well as the effect of grouting. All four walls, therefore, had a gross vertical reinforcement ratio (ρ_s) of 0.26% and the sectional properties listed in Table 1. Walls W1CG and W2NSG were fully grouted, Wall W3CPG had $1/3^{rd}$ of cores grouted, and Wall W4NSU remained hollow as shown in Figure 2.

Table 1: Test Wall Sectional Properties

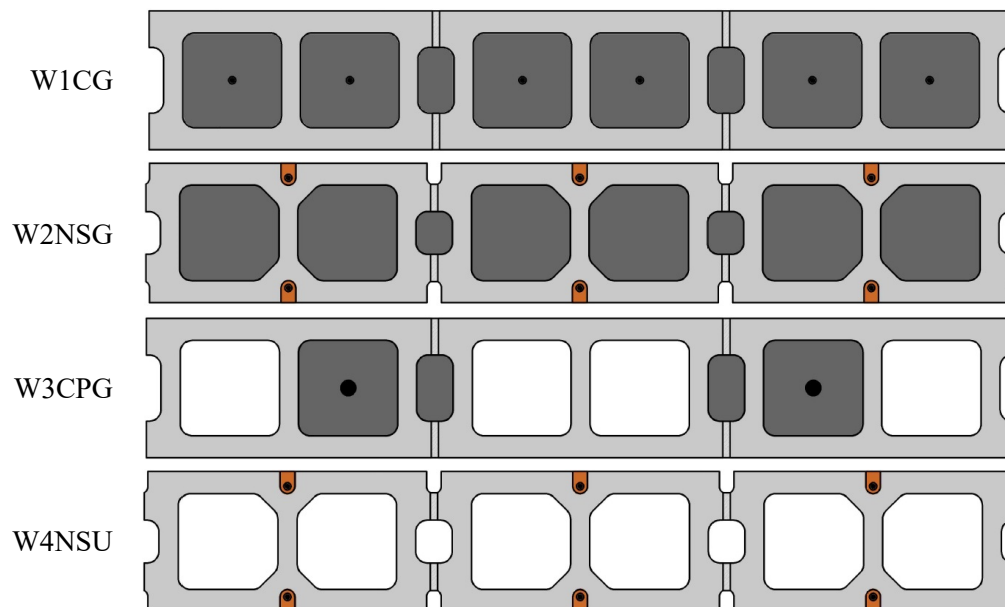| Wall ID	ρ_s [%]	Grouted cores [x/6]	Bar size (quantity)	Depth to tension reinforcing bar [mm]	Area of steel in tension [mm²]
W1CG	0.26	6	10M (6)	95	600
W2NSG	0.26	6	10M (6)	170	300
W3CPG	0.26	2	20M (2)	95	600
W4NSU	0.26	0	10M (6)	170	300

Figure 2: Typical Test Wall Cross Sections

The height of each wall was 3.2m (16 courses) to represent a one-storey masonry wall. The length of each wall was 1.2m to ensure stability during construction and allow reinforcement patterns to be repeated along the length.

Test Set-up
The test set-up, was modeled after Abboud et al. [1]. Pin and roller connections at the bottom and top of the wall, respectively, were achieved by connecting an axle through a series of pillow block ball bearings. Loads were applied uniformly across the length of the wall along two lines located at third points along the height of the walls. Loads were applied monotonically until failure. Failure was defined as a 20% drop in the out-of-plane flexural resistance due either to crushing of the masonry under compression, or shear, or fracture of the reinforcing bars.

FINITE ELEMENT MODELING
To complement the experimental testing of the reinforced wall specimens, a finite element (FE) model was constructed for each wall. These models were then analyzed under the same conditions as those described for the walls tested. The FE models and the analyses were corroborated based on results previously reported by Sparling [5]. Although the properties of the materials (masonry units, steel, mortar, and epoxy) may vary significantly from the values previously reported, the analyses of the conventionally-reinforced walls and the walls with NSM reinforcement are used to better understand contrasting behaviours prior to testing. Furthermore, these models will be corroborated and refined through the test program and then used to conduct parametric studies of salient response parameters.

For this purpose, the ATENA 3-D FE analysis package was employed. A 3-dimensional analysis was used in this study given that the voids and thin webs of hollow CMUs would not be accurately represented in a 2-dimensional environment. The ATENA package was selected for its capacity to analyze the cracking behaviour of reinforced concrete and masonry systems.

Material Models
Individual material properties were assigned to the CMUs, mortar beds, grout, and reinforcing steel to accurately represent the interaction of the various materials that constitute a reinforced masonry system. The CMUs, mortar, and grout were modeled using a 3-dimentional non-linear cementitious constitutive model. Steel reinforcement elements were modeled as 2-dimentional truss elements with a bilinear stress-strain relationship. Support and loading elements (steel plates) were modeled using a 3-dimentional, linear-elastic isotropic constitutive model. A summary of the critical properties assigned to the various materials is listed in Table 2. These properties were selected based on data recorded previously [5] and on recommended values from Drysdale and Hamid [6].

Table 2: Constitutive Models – Summary of Properties

Material	Constitutive model type	Properties
Concrete block (CMU)	3-D non-linear cementitious	f'_c=25MPa E=18.5GPa f_t=2.3MPa μ=0.2
Mortar	3-D non-linear cementitious	f'_c=10MPa E=12GPa f_t=0.8MPa μ=0.2
Grout	3-D non-linear cementitious	f'c=12MPa E=18.5GPa ft=1.3MPa μ=0.2
Steel plate	3-D linear-elastic isotropic	E=200GPa μ=0.3
Steel rebar	2-D bilinear	f_y=400MPa E=200GPa

To limit the complexity of the assembled models, a perfect bond was assumed between adjacent elements. However, to avoid over-estimating the tensile strength of mortar joints, the tensile strength of the mortar material was set to lie within the range of tensile bond strength reported in Drysdale and Hamid [6]. In this way, the masonry units were effectively bonded to each other with the bond strength typical of a masonry-mortar bond. A perfect bond was assumed between the steel reinforcing bars and the surrounding material.

Model Geometry
The geometric properties of the FE models were simplified from the properties of the as-built walls. The simplifications resulted in a reduction in the number of elements necessary to accurately model the geometry, and to allow the meshing of the models using only brick-type elements. Each wall was separated into 7 components, each having similar properties across all four wall models. These components consisted of the following: compressive CMU face shell, tensile CMU face shell, mortar joints in tension, CMU webs, grouted cores, steel reinforcement, and steel supports and load spreader beams. The components were assembled as shown in Figure 3 where the bottom support and first course of Walls W3CPG and W4NSU are represented.
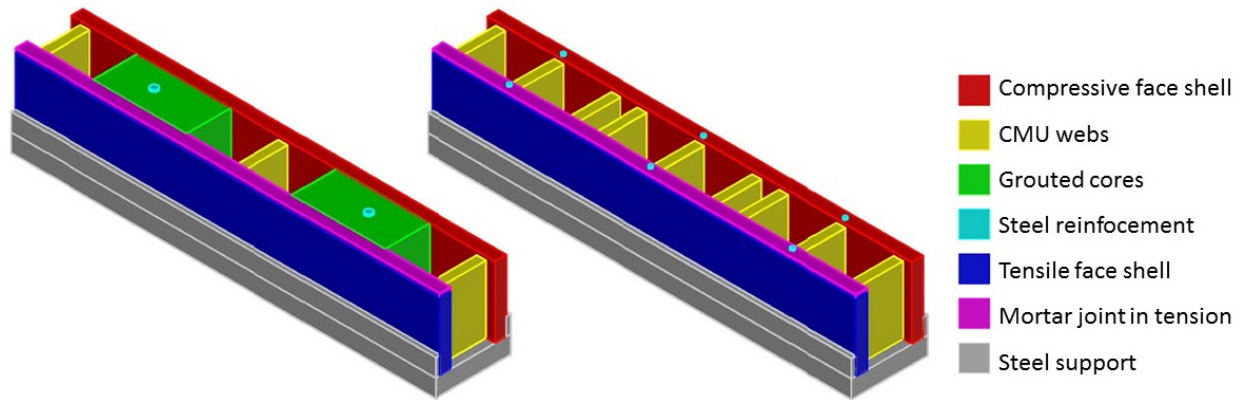
Figure 3: FEM of the First Course W3CPG (left) and W4NSU (right)

The compressive face shell of each wall was modeled as a single monolithic component with the properties of the concrete block. This component, therefore, had a thickness of 32mm, a width of 1200mm, and a height of 3190mm. Since no tensile cracks are expected on the compression face of the wall, the behaviour will be governed by the properties of the CMU. Furthermore, the compressive properties of the CMU used for the analysis were assigned based on axial testing of masonry prisms. Since the compressive properties of mortar were accounted for within the material model for the CMU, it was deemed unnecessary to include mortar joints on the compressive side, and they were lumped into the face shell. Although localized crushing at the mortar joints in compression is possible, that effect was not considered in this analysis.

The tensile face of each wall was modelled as successive courses of CMU face shell and horizontal mortar bed. The CMU face shell elements each had a thickness of 32mm, a width of 1200mm and a height of 190mm, while the mortar beds had the same thickness and width, but a height of only 10mm. These successive layers of material with different tensile strength create the preferential planes of horizontal cracks typical of masonry construction. Head joints are not expected to greatly impact the behaviour of the walls, and were, therefore, not included in the FE models.

The CMU webs spanning from the compressive face to the tensile face were modeled as three separate components for each CMU. These components each had a thickness of 26mm, a length of 126mm, and a height of 190mm, and were spaced to match the location of webs in the walls as built. There was, therefore, no vertical continuity between the webs of successive courses, as is the case in the walls as built.

Grouted cores, when applicable, were modelled with components spanning the entire grouted width including adjacent webs, and the full height of the wall. To simplify the models, the CMU webs were deleted from locations containing grout since the average mechanical properties in those areas are expected to closely resemble that of the grout.

Mesh Size and Analysis Steps

The mesh sizes for the various components of the models were selected to be as coarse as possible while limiting the aspect ratio of elements to 2:1. All components were therefore meshed with elements having a maximum length in any direction of 40mm. This size results in an aspect ratio greater than two for elements in the mortar joints; however, since they are expected to crack at relatively low load levels, their larger aspect ratio is not expected to have a significant influence on the analysis results. The models were analyzed under monotonic loading in increments of 0.5mm until failure.

Model Validation

A model of the reinforced masonry flexural specimens from Sparling [5] was constructed and analysed using the material models and meshing described above. The load-deflection results, under third-point loading, of the analysis and the data from Sparling [5] are shown in Figure 4. Specimens F1, F2, and F3 were replicate hollow walls, each constructed from six stack bonded SCRMU units with a single steel reinforcing bar bonded into the central groove on both exterior faces. Up to a load of approximately 12kN, the numerical load-deflection curve captures the un-cracked stiffness of the masonry assembly; however, during testing, the mortar joints separated from the CMUs at the onset of loading and the un-cracked response was not observed. This was attributed to the weak CMU-mortar bond achieved in the specimens due to the method by which the units were manufactured. Agreement between the results at loads above 15kN suggests that the selected constitutive models, model geometry, and element mesh accurately simulate the cracked flexural behaviour of the reinforced masonry assemblies. It should, however, be noted that the FEA model predicted failure due to crushing of the masonry in compression, whereas the observed failure was diagonal shear tension.
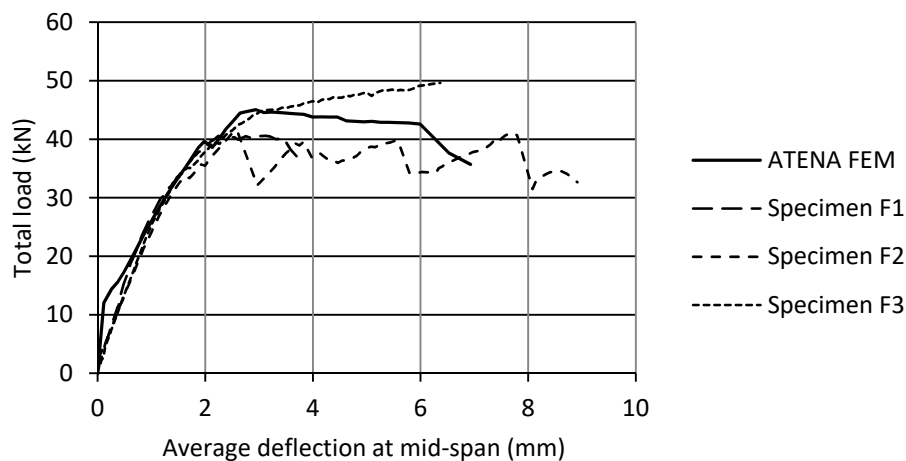

Figure 4: Load-Deflection Results for ATENA FEM and Reinforced Walls from Sparling [4]

FINITE ELEMENT ANALYSES

The load-deflection results of the FE analyses for the two fully grouted walls and two hollow walls of the present study are shown in Figure 5 and Figure 6, respectively. These results highlight the difference in behaviour between walls with conventionally placed reinforcing bars, and those with NSM reinforcement. The shape of the load-deflection curves for grouted walls shown in Figure 5 closely matches that of grouted walls tested by Abboud et al in [1], suggesting that the material model used to represent the grout reasonably simulates the behaviour.
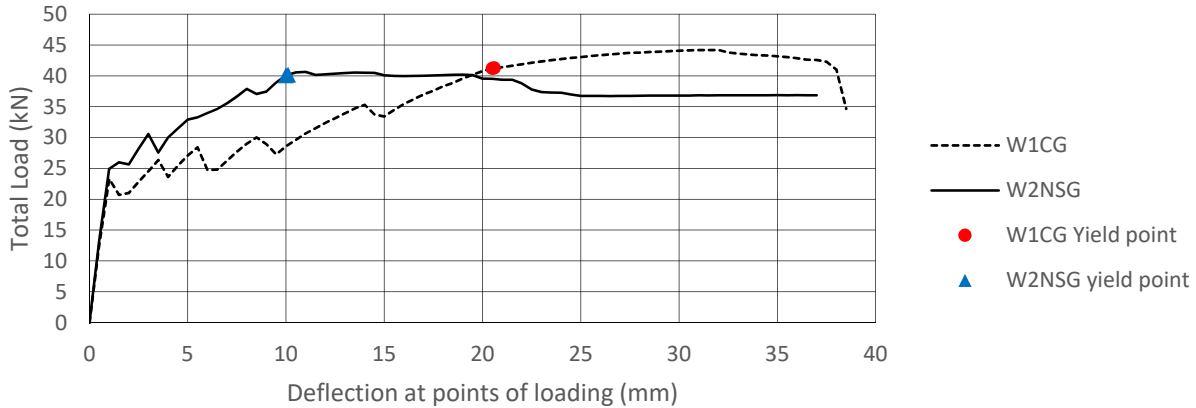

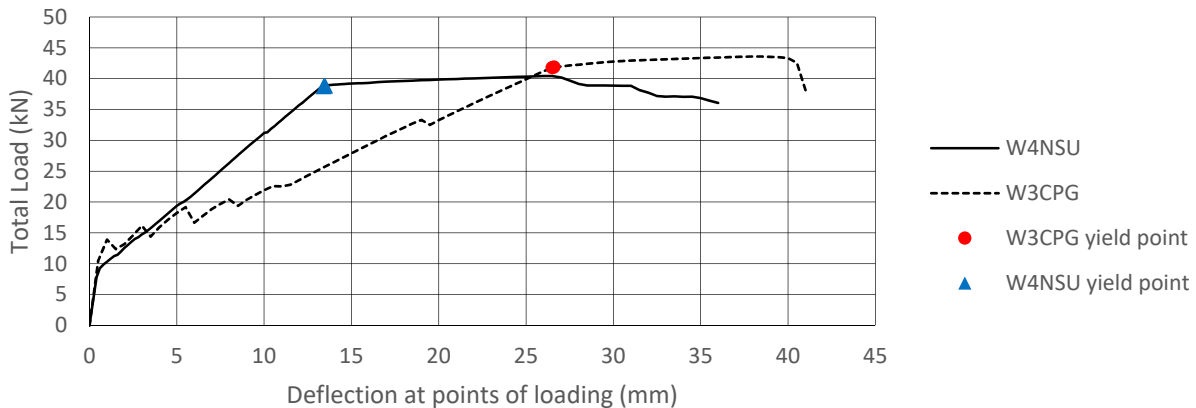**Figure 5: Load-Deflection for Grouted Walls W1CG and W2NSG**

Figure 6: Load-Deflection for Hollow Walls W3CPG and W4NSU

Walls W1CG and W2NSG demonstrate similar flexural behaviour up to approximately 60% of the ultimate load. For loads up to 60% of ultimate, the behaviour is controlled by the tensile strength of the grout (un-cracked behaviour). For loads beyond 60% of ultimate, the sections begin to crack and flexural behaviour is controlled by the reinforcing bars. The cracked section with conventional reinforcement, W1CG, exhibits significantly lower stiffness than W2NSG. Furthermore, the reinforcing bars begin to yield in tension after a deflection of 10mm for

W2NSG, whereas the reinforcing bars in Wall W1CG yields after 20mm of deflection. The onset of yielding corresponded to the load at which the strain in the reinforcing bars exceeded 0.2%.

Similar differences exist between Walls W3CPG and W4NSU. The un-cracked stiffness of the walls are similar, however W3CPG exhibits significantly lower post-cracking stiffness. The onset of yielding of the reinforcing bars also occurs at a significantly higher deflection for Wall W3CPG (27mm) than Wall W4NSU (13mm). Additionally, since these walls contain less cementitious materials in tension, the cracking load is less than half that of the fully grouted walls.

Another notable difference between the conventionally-reinforced walls and those with NSM reinforcement is the level of cracking in the walls at the onset of yielding of the longitudinal steel in tension. The onset of yielding generally represents the point at which further deformation is not recoverable. It therefore represents the maximum load level at which the structure could be expected to maintain its functionality.

Figure 7 illustrates the deflected shape of the four models magnified 5-fold at the onset of yielding. Locations with significant normal tensile stress are depicted in red, locations with high compressive stress are noted in blue. The black lines indicate cracks wider than 0.2mm. Table 3 summarizes the load, average deflection at the loading points, and secant stiffness at states matching those shown in Figure 7. The ductility capacity, defined as the ultimate deflection (Δ_{ult}) divided by the deflection at the yield point (Δ_y), for each wall is also shown.
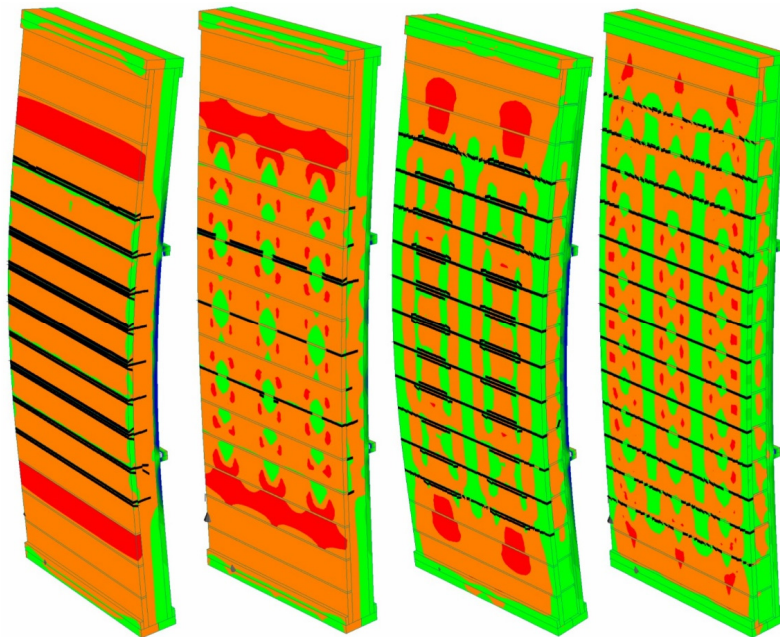

Figure 7: Normal Stress and Crack Pattern at Onset of Yielding of Walls W1CG, W2NSG, W3CPG, and W4NSU (From Left to Right)

Table 3: Load and Deflection Values at the Onset of Reinforcement Yielding

Wall ID	Load (kN)	Deflection at point of loading (mm)	Secant Stiffness (kN/mm)	Ductility Capacity (Δ_{ult}/Δ_y)
W1CG	41.2	20.5	2.0	1.85
W2NSG	40.1	10.0	4.0	3.70
W3CPG	41.8	26.5	1.6	1.55
W4NSU	38.8	13.4	2.9	2.69

Comparing the behaviour of W1CG to that of W2NSG, and the behaviour of W3CPG to that of W4NSU, if becomes evident that the walls reinforced with NSM reinforcement exhibit lower stress in the masonry and decreased severity of cracking at the onset of yielding.

DISCUSSION

The walls with NSM reinforcement have an ultimate strength within 10% of that of equivalent conventionally-reinforced walls. However, the FE analyses suggest that the NSM-reinforced walls have approximately half the level of deflection of conventionally-reinforced walls at the onset of yielding of the longitudinal reinforcement in tension. Furthermore, the NSM-reinforced walls exhibit significantly higher ductility than conventionally-reinforced walls.

Since masonry walls are designed to behave as a cracked section when in service, these FE analyses clearly illustrate the benefits of using NSM reinforcement over conventional reinforcing techniques. The increase in stiffness of these walls will result in decreased cracking during service as well as a reduction in the P-Δ effects for tall walls and walls with large axial loads.

The numerical results, presented herein, are preliminary and will be validated with future experimental data. The proposed testing will provide the necessary data to modify the modelling to capture aspects of behaviour that may not have been fully captured by the FE models. This includes the effects of shear sliding, bond-slip of the reinforcing bars, local crushing of mortar, or buckling of the NSM reinforcement in compression.

CONCLUSIONS

NSM reinforcing bars may be used to reinforce masonry walls constructed from specially manufactured SRCMUs. FE models comparing three-metre tall conventionally-reinforced walls to walls having the same dimensions, effective area, and reinforcement but reinforced with NSM bars suggest that the latter have significantly higher cracked stiffness and a higher ductility capacity. Furthermore, the flexural strength of the NSM-reinforced walls is within 10% of that of conventionally-reinforced walls both at the onset of yielding and at the state of maximum load. The numerical analysis results will be compared to experimental data from testing performed on full-scale walls of the same materials and dimensional details.

REFERENCES
[1] Abboud, B. E., Hamid, A. A. and Harris, H. G. (1996). "Flexural Behavior of Reinforced Concrete Masonry Walls Under Out-of-Plane Monotonic Loads." *ACI Structural Journal,* 93 (3): 327-335.
[2] Dizhur, D., Griffith, M. and Ingham, J. (2014). "Out-of-Plane Strengthening of Unreinforced Masonry Walls using Near Surface Mounted Fibre Reinforced Polymer Strips." *Engineering Structures*, 59: 330-343.
[3] Tumialan, J. G., Micelli, F. and Nanni, A. (2001). "Strengthening of Masonry Structures with FRP Composites." *Proc., Structures 2001: A Structural Engineering Odyssey*, Washington, DC, USA, May 21-23, http://ascelibrary.org.
[4] Sparling, A. J. J., Hashemian, F. K. and Britton, M. G. (2015). "Surface Reinforced Concrete Masonry Units: An Introduction to the Future of Concrete Masonry." *Proc., CSCE 2015: Building on our Growth Opportunities*, Regina, SK, Canada, on USB.
[5] Sparling, A. J. J. (2015). "The Development of a Hollow Concrete Masonry System for use with Near-Surface Mounted Reinforcement." MSc thesis, University of Manitoba.
[6] Drysdale, R. G. and Hamid, A. A. (2005). *Masonry Structures Behaviour and Design*, Canada Masonry Design Centre, Mississauga, ON, Canada.